Improved calculations of interplanetary magnetic field phase front angles and propagation time delays

Daniel R. Weimer[1] and Joseph H. King[2]

Received 4 April 2007; revised 2 August 2007; accepted 28 September 2007; published 31 January 2008.

[1] It has been known that the variations in the interplanetary magnetic field (IMF) occur within surfaces that are tilted with respect to the solar wind velocity vector. This tilting of the IMF phase fronts may cause the propagation from a point of observation to another location to have delay times that vary substantially. Therefore for accurate delay calculations in real time, or for the creation of scientific data sets, it is necessary to be able to determine the phase surface orientation angles using the magnetic field measurements on one spacecraft only. Methods for calculating these tilt angles have been tested for accuracy by a comparison using IMF measurements on multiple satellites. One method is a variation of the minimum variance of the magnetic field, where it is constrained by the condition that the average field along the phase front's normal vector is zero. This method is referred to as MVAB-0. Another technique is to simply calculate the vector cross product between magnetic fields measured at two different sample times. The choices of the different parameters for the calculation and error discrimination are important. An optimization of parameters was done by testing how well the propagation delays from one spacecraft to others are predicted. The tests have indicated that, when optimized, both procedures work comparably well. It had also been found that further improvements to time delay predictions are obtained by combining together both the MVAB-0 and cross-product techniques, where the results of both methods must be in near agreement.

Citation: Weimer, D. R., and J. H. King (2008), Improved calculations of interplanetary magnetic field phase front angles and propagation time delays, *J. Geophys. Res.*, *113*, A01105, doi:10.1029/2007JA012452.

1. Introduction

[2] From multiple-satellite measurements of the interplanetary magnetic field (IMF), and the timing of IMF transitions arriving at the different satellites, it has been known that the variations in the magnetic field typically occur within surfaces that are tilted with respect to the solar wind velocity vector. If the IMF is measured at a particular location in the solar wind, such as on the NASA Advanced Composition Explorer (ACE) satellite at the first Lagrangian (L1) orbit, it is necessary to calculate the propagation delay time to determine the arrival of the same field vector at a location downstream in the solar wind. The tilting of the IMF "phase fronts" may cause the actual delay time to be different from what would be otherwise expected if a nontilted propagation is assumed, particularly between points that have a large offset in the GSE Y and/or Z directions [*Collier et al.*, 1998; *Weimer et al.*, 2002]. The determination of phase front orientations by intersatellite time delays cannot be done in real time, and it is rarely possible to have three or more satellites taking simultaneous IMF measurements in the solar wind. Therefore it is necessary to be able to determine the phase front normal (PFN) orientation angles using the magnetic field measurements on one spacecraft only, such as ACE, particularly if real-time IMF measurements are to be used for downstream space weather predictions.

[3] *Weimer et al.* [2003] had found that a minimum variance technique [*Sonnerup and Scheible*, 1998] may be used successfully for calculating the IMF phase front orientation with measurements at a single location, such as at the ACE spacecraft, as long as a sufficiently large number of points was used for each "variance matrix" calculation. In a correction by *Weimer* [2004] it was noted that the technique worked only due to a serendipitous program error, which calculated a "modified variance matrix." *Bargatze et al.* [2005] established that this modified variance matrix was actually calculating an approximation to the minimum and maximum variance directions with respect to the mean magnetic field vector as averaged over the analysis interval. The approximation is valid if a large number of points are used, as was the case. They proposed an exact, rather than approximate, calculation such that "to find the plane normal one can first solve for the IMF variations perpendicular to the long-term mean field direction," and then calculate the variance matrix by the conventional minimum variance equation. In a subsequent comment paper, *Haaland et al.* [2006] suggested that

[1]Solana Scientific, Brookline, New Hampshire, USA.
[2]Perot Systems and NASA Goddard Space Flight Center, Greenbelt, Maryland, USA.

Copyright 2008 by the American Geophysical Union.
0148-0227/08/2007JA012452

a better way is to use a variation of the minimum variance of B, such that it is constrained by the condition that the average field along the minimum variance direction (the PFN) is zero. *Sonnerup and Scheible* [1998] had discussed this method, referred to as MVAB with constraint $\langle \mathbf{B} \rangle \cdot \hat{\mathbf{n}} = 0$. *Sonnerup et al.* [2004] and *Haaland et al* [2004] refer to this calculation using the acronym MVABC, whereas *Haaland et al.* [2006] use the term MVAB-0. This later convention will be used through the remainder of this paper. In the reply by *Bargatze et al.* [2006], it was noted that the results from MVAB-0 are exactly identical to the technique that the original *Bargatze et al.* [2005] paper had suggested, even though the methods of calculations are different.

[4] Neither the method proposed by *Bargatze et al.* [2005] nor the MVAB-0 technique proposed by *Haaland et al.* [2006] had been tried with any significant amounts of IMF data and actual time delay calculations. Only one "benchmark interval" was published for the variance matrix calculations, producing just one data point. So the question remains, how well can either equivalent method perform with determining the PFN angles, as a continuous function of time, with a continuous stream of IMF measurements? Also, what are the optimal parameters to use, such as the number of data points to use in the calculation of each variance matrix?

[5] In a relevant study of discontinuity observations by *Knetter et al.* [2004], discontinuity normal vectors were derived by triangulation of four-point satellite crossings through discontinuities, using magnetic field data from the Cluster satellites. They had found that a cross-product method generally produced better matches with triangulation than using MVA with the constraint that B-normal is small. In this cross-product technique the direction that is normal to the surface of the IMF transition is found simply by taking a cross product of two averaged magnetic field vectors positioned upstream and downstream of the transition. The *Knetter et al.* [2004] study was concerned with well-defined discontinuities in the IMF, rather than having any concern for a steady stream of ordinary IMF variations. Even so, is it possible that a cross-product method could be used for a continuous PFN determination?

[6] The purpose of research described in this paper is to answer the questions that have been raised. The objective is to determine which methods work the best for PFN and time delay calculations and to also find out how to optimize each technique. To be practical for the creation of propagated IMF data sets, as well as a real-time forecasting tool, the methods and parameters chosen must work with a continuous stream of ordinary IMF measurements, rather than being concerned with a detailed analysis of well-defined discontinuities.

2. MVAV-0 Calculations

[7] The standard minimum variance calculation is accomplished by calculating the three-by-three variance matrix from a set of magnetic field vector measurements:

$$M_{ij} = \langle B_i B_j \rangle - \langle B_i \rangle \langle B_j \rangle \tag{1}$$

Next the three eigenvalues λ_1, λ_2, λ_3 of this matrix are calculated, as well as the corresponding, orthogonal eigenvectors, $\boldsymbol{x}_1$, $\boldsymbol{x}_2$, and $\boldsymbol{x}_3$. The three eigenvectors represent the directions of maximum, intermediate, and minimum variation of the field components [*Sonnerup and Scheible*, 1998]. The eigenvector that corresponds to the smallest eigenvalue (EV) is in the direction of minimum variance, which is normal to the surface that contains the discontinuity or phase front. The ratio between the intermediate and minimum eigenvalues is often used as an indicator of the quality of the PFN determination, where the result is either used or discarded.

[8] As mentioned earlier, the MVAB-0 variation is constrained by the condition that the average field along the minimum variance direction (the desired PFN) is zero. *Haaland et al.* [2006] point out that in the easiest implementation of the MVAB-0 method, attributed to A. V. Khrabrov by *Sonnerup and Scheible* [1998], the first step is to obtain the "projection matrix" P:

$$P_{ij} = \delta_{ij} - \hat{e}_i \hat{e}_j \tag{2}$$

where δ_{ij} is the Kronecker delta and the unit vector $\hat{\mathbf{e}}$ is in the direction of the average magnetic field vector. The matrix P describes a projection of a vector onto a plane perpendicular to $\hat{\mathbf{e}}$. Next the M matrix is multiplied on both the left and right sides by this projection matrix P:

$$Q_{nk} = P_{ni} M_{ij} P_{jk} \tag{3}$$

To solve for MVAB-0, the eigenvectors and eigenvalues are determined for this matrix Q, rather than M. The smallest eigenvalue of this Q matrix is exactly zero, and the corresponding eigenvector is in the direction of the average magnetic field. The nonzero, maximum, and intermediate eigenvalues are used in the ratio which determines the quality of the result.

[9] There are no firm guidelines for how many data points to use for constructing each variance matrix, particularly if the method is to be used with a continuous stream of data for a forecast tool, rather than postevent analysis of a well-defined event such as a known tangential discontinuity or a magnetopause crossing. Likewise, the "goodness test" with the eigenvalue ratios has no absolute rule for what cutoff value to use for discriminating between the good and indeterminate results. Resolving these questions was another objective of this project.

[10] For the purpose of comparison the process described by *Bargatze et al.* [2005] and the MVAB-0 calculation were both implemented in programs for processing a continuous stream of IMF measurements. It was confirmed that the two methods do produce identical results at every data point, although the MVAB-0 algorithm did prove to be computationally more efficient (i.e., faster) to implement in a vector-processing language such as Research System's Interactive Design Language (IDL). One other difference that was noticed is that in programming the Bargatze procedure it is possible to calculate the "long-term mean field direction" using a running average with a number of points that is different from the number of points used to construct each variance matrix. Only when the running average is calculated from exactly the same number of points as the variance matrix are the results exactly the same as

MVAB-0. As the MVAB-0 matrix algorithm was more efficient, this calculation was used for the remainder of the tests described here.

3. Cross-Product Method

[11] The cross-product method works simply by taking a vector cross product of average magnetic field vectors both upstream and downstream of a discontinuity [*Burlaga*, 1969; *Horbury et al.*, 2001; *Knetter et al.*, 2004]. When used with a continuous stream of IMF measurements, rather than a known discontinuity, this calculation is applied at every point in the series, and the results are used only if certain criteria are met. The primary criteria is that the angle between the magnetic field vector upstream and downstream, that Knetter et al. refer to as the "spreading angle ω," must be sufficiently large. This angle ω is obtained directly from the cross-product calculation, and Knetter et al. report that its use dates back to "the first operational definition of a directional discontinuity (DD) given by *Burlaga* [1969]."

[12] What number to use as the cutoff for a sufficiently large spreading angle is one of the parameters that had to be determined by further testing with continuous IMF. There are other variables too, such as the number of points to use for calculating the average magnetic field vectors for the cross product. The spatial/temporal separation, or number of data points N, between each vector in the calculation is yet another variable, as it does not need to be the same as the number of points in each field average. As implemented in these tests, the IMF for each day is first smoothed by a running, "boxcar" average, while retaining the original sample spacing. Then the day is processed one point at a time in sequence. At each point the cross product is obtained from the two average vectors that are located at plus and minus N data points from the center; the result is used for a phase front normal determination only if the spreading or rotation angle is greater than a predefined limit.

[13] During the early tests of the cross-product method it was determined that an additional constraint on the results should be introduced, based on the MVAB-0 model. As B-normal should be close to zero, there was added a requirement that the cross-product result, normalized and taken in a dot product with the average magnetic field unit vector at the center point, should be less than some small value, to be determined. In all there are four variable parameters to be optimized.

4. Testing With Multiple-Spacecraft Measurements

[14] Initially, the tests of the single-spacecraft, phase front calculation methods were conducted by a comparison of the PFN direction angles with those obtained from simultaneous, four-satellite IMF measurements. The PFN direction angle as a function of time are determined by measuring the continuously varying propagation delays between ACE and the Wind, Geotail, and IMP-8 spacecraft, for cases where all four spacecraft were located within the interplanetary field. The technique is described in more detail by *Weimer et al.* [2002], where the time delays are measured by determining the time shifts that produce the best match-up of the various features in the IMF that are measured on the different spacecraft. For these more recent tests the delay measurement method was first improved from the 2002 version with a higher temporal resolution in the phase-matching algorithm.

[15] The comparisons were done by running the single-spacecraft phase front calculation routines for periods within 38 different days to produce a "prediction" of PFN direction angles as a function of time. The "Level 2" science data from the magnetometer on ACE were used, having a time step of 16 s between each vector measurement [*Smith et al.*, 1998]. A score for each MVAB-0 or cross-product test run (with different parameters for the PFN calculations) was computed from the mean of the total square difference between the PFN direction angles and the PFN angles obtained with the multiple-satellite, delay-measurement method. The comparison was done only for the time periods within these 38 d where the four-satellite determination had a relatively low error, as indicated by how well the results could be fit to a planar surface (for details, see *Weimer et al.* [2002]). This test also excluded time periods on 5 of the days when Geotail was within the bow shock rather than solar wind. Other periods were excluded when the time-delayed positions of the satellites were such that they were all nearly colinear, which precludes the determination of a unique orientation for a plane. A dot product of the plane-normal vectors was used to indicate how well the two methods matched.

[16] These tests were mainly concentrated on the MVAB-0 method, as it was of particular interest to find the optimal value for the minimum allowed value of the ratio between the intermediate and minimum eigenvalues in each variance matrix calculation. Variance calculations with ratio below this cutoff value are assumed to be unreliable and discarded, so it is desirable to know what ratio value will distinguish between the good and bad PFN calculations. Although there was found to be a good correlation between the eigenvalue ratios and how well the minimum variance eigenvectors matched the four-satellite PFN determinations, there simply does not exist any one, well-defined cutoff ratio that sorts between the vectors that matched (dot product close to one) and those that did not. In most cases an eigenvalue ratio cutoff values in the range of 3 to 5 generally produce the best compromise, yet nevertheless result in some well-matching results to be discarded. Other parameters, such as the number of points to use in the variance matrix or cross-product calculations were tested by means of these PFN angle comparisons.

5. Tests With Time-Delay Propagation

[17] As there was no way to independently verify the accuracy of the PFN measurements from the multiple-satellite time delay method, it was decided to move on to an alternative technique for testing and optimizing the PFN calculation methods. The various techniques were used in programs that would process the ACE IMF measurements and use the PFN determinations to calculate the propagation delays from ACE to other satellite locations, such as Wind, IMP-8, and Geotail. The solar wind velocities that are

required for the delay predictions are measured by the Solar Wind Electron, Proton, and Alpha Monitor (SWEPAM) on ACE [*McComas et al.*, 1998].

[18] These programs produce predictions of the IMF as a function of time at the "target" locations in the downstream solar wind. Further refinement of the best values to use for the different parameters in the prediction routines are achieved by comparing these delayed IMF predictions from ACE with the values measured on the other satellites in the IMF. A score for the relative merit of each method was obtained by totaling the square of the difference between the predicted and measured values, using all three components of the IMF vectors. Each score was computed using the results from 38 different days, comparing the predictions from ACE with the measurements on both the Wind and IMP-8 spacecraft between 0100 and 2300 UT on each of the days, excluding data gaps. The total of the square error from every point in the comparison was then divided by the total number of measurements, times three, to obtain the figure of merit. For the purpose of comparison with the 16-s ACE data, the 3-s Wind data were averaged and resampled at 15 s resolution and IMP-8 data had a resolution of 15.36 s.

[19] For the purpose of calculating time delays as a continuous function of time, there are different options for handling the intervals in which there are no updates to the tilt angles. One method is to keep the tilt angle fixed at the previous value until a new angle is found, then changing it to the new value with a step change. Another option is to interpolate the tilt angles in the intervals between the measurements that pass the selection criteria. This second option tends to produce better test scores as well as smoother graphs and has been used in our post-2003 work.

[20] The calculation of the downstream IMF values after applying the propagation delay times is another matter. If IMF values are measured with instrumentation on ACE at times t_1 and t_2, where t_2 follows t_1, then if there is a sudden decrease in the propagation delay time between t_1 and t_2, due to a change in the PFN angle, then it is possible for IMF_2 to be predicted to arrive at the downstream target satellite earlier than IMF_1 rather than later, even if the velocity does not change. This result seems to be a nonsensical, as it is unlikely that the phase surfaces simply propagate through each other. The apparent contradiction is simply due to geometrical effects. Since the phase surfaces with different tilt angles are not parallel they will intersect at some distance away from ACE, in a direction perpendicular to the solar wind vector. They will not intersect directly downstream from ACE. On scales of several tens of R_E the phase surfaces appear to be nearly planar, but at larger scales they have some curvature, so they may actually curve away from each other at large distances instead of intersecting. Furthermore, *Borovsky* [2006] has proposed that the IMF "discontinuities are interpreted to be the walls of independently moving magnetic flux tubes (plasma tubes) with a large spread of orientations about the Parker-spiral direction," and shows conceptual diagrams of these flux tubes as having a multitude of scales and being intertwined. Having finite lengths in the Y or Z direction, some surfaces that move by ACE may pass over or under each other at some distance away from ACE, and their associated IMF signature may not even be detected at other spacecraft, so only IMF_1 or IMF_2 is seen rather than both. Another possibility is that the magnetic fields associated with two intersecting phase surfaces may merge together, forming a region with a different orientation.

[21] This still leaves us with the problem of how to deal with what we call "out-of-sequence arrivals" when predicting the downstream IMF as a linear function of time. Various methods have been tried to deal with the problem, such as giving the measurements that arrive out of sequence late a precedence over earlier measurements or doing the opposite and ignoring the late arrivals. These methods amount to assuming that the phase surfaces may or may not overlap the downstream ones at the Y/Z offset positions. An alternative is to simply sort the downstream IMF values into sequential order according to their arrival time tags. This propagation method has been found to produce the best test scores, as noted at the end of section 8. For the earlier or later IMF to have priority, either way is possible at some downstream location, but it cannot be known in advance from our limited data on ACE alone, so it works best to not favor one or the other.

[22] The IMF measurements that originally have a fixed time cadence, 16 s in the case of ACE, have predicted arrival times at a random order and spacing. For graphs and comparison with the target satellites' IMF measurements, the next step is to resort the arriving time tags, and associated IMF measurements, into sequential order. These may be graphed in this sorted order as a function of time or compared directly with the target measurements, using an interpolation between the nearest time tags. A better alternative is to first resample/average the propagated values to evenly spaced, ~15-s time intervals, matching the resolution of the data at the target spacecraft, before doing the interpolation. If more than one propagated IMF sample is calculated to arrive within the range of one time interval, then the vector components are averaged together. Time intervals are filled by interpolation if they have no time-shifted ACE data arriving within them. This resampling and averaging procedure produces both better looking graphs and improved test scores. This averaging method is also consistent with the possibility that the IMF associated with intersecting surfaces may merge together, with the merged IMF having an intermediate orientation.

6. MVAB-0 Parameter Optimization

[23] The figure of merit test score was computed for various combinations of parameters for the MVAB-0 method in order to determine which are optimal for use with the IMF. A grid containing a wide range of values for each input parameter was initially used. After computing the score for every point on the grid, the process was repeated with smaller steps for each parameter, centered on the previous combination that produced the best score (lowest error). This process was repeated until the grid spacing was at the desired resolution for all variables. The grid point with the best score showed which combination of parameters to use for the IMF.

[24] Figure 1 shows the test scores for the initial grid, where the number of points in each matrix calculation

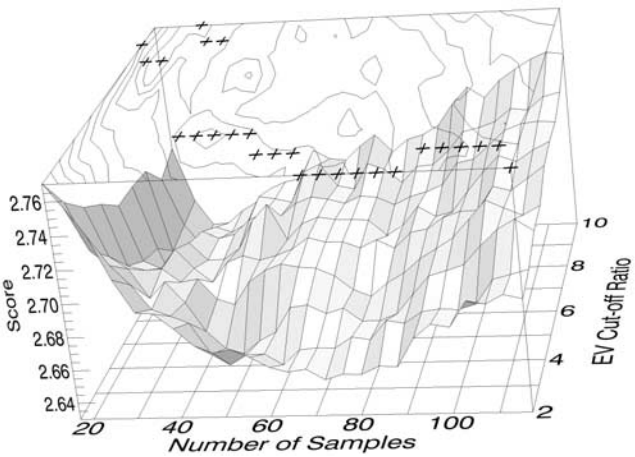

Figure 1. Test scores for the MVAB-0 method using a range of two parameters on a grid. One axis has the number of samples used for each variance matrix calculation, and the other axis is the cutoff ratio for the eigenvalue ratio. The mean square error for 38 d, using data from the ACE, Wind, and IMP-8 spacecraft, is represented by the vertical surface and the superposed contour graph. The cross marks on the contour graph indicate which cutoff ratio had the lowest, best score for each number of samples. The lowest point is found at (25, 8).

varied between 17 and 117 and the minimum cutoff value for the eigenvalue ratio was in the range of 2 to 10. The low score is 2.630 nT^2, at 25 points and a cutoff ratio of 8. Further iterations at higher resolution resolved the low point to be at 2.624 nT^2, at 25 points and a cutoff ratio of 7.8. These results are derived using the resampling and averaging of the propagated IMF. If the resampling/averaging process is skipped before the final comparison with the target IMF, then the error surface that results (i.e., a graph like Figure 1) is more irregular. Additionally, without the final averaging step the best score value is larger (2.699 nT^2) and found at a different location (77 points, 5.2 ratio).

[25] The time delay predictions have another parameter that could be varied in the tests, and this is the "limit angle" for each calculated PFN direction [*Ridley*, 2000; *Weimer et al.*, 2003]. Each calculation of the PFN angles must have an angle with respect to the solar wind velocity vector that is less than the limit angle, otherwise unrealistic delay times are introduced. The limit angle that produces the best match between the time-delayed ACE measurements and the IMF at the target satellites was found to be 75°.

[26] The differences between test scores seen here may appear to be small, but keep in mind that these are averages that are derived from about 300,000 vector samples, and the delay estimations only have an effect on the outcome at the minority of points surrounding IMF transitions. Every change in the IMF at which the phase surface angle measurement and propagation time estimate are improved contributes to a better score.

7. Cross-Product Parameter Optimization

[27] As mentioned earlier, the cross-product method has four parameters, corresponding to the number of points to use for IMF smoothing prior to the calculation, the point separation between cross-product vectors, the minimum spreading angle, and the maximum allowed B-normal value. Therefore the optimization tests were done on a four-dimensional grid, having no simple graphical representation. After repeated iterations, the best score for the cross-product method, 2.615 nT^2, was obtained by first smoothing the IMF measurements with a 19-point running average, then calculating the cross product at each time step using the (smoothed) vectors at plus and minus 4 steps (8 total), with a separation of 128 s. The cross-product results then had to have a rotation or spreading angle of at least 8.8 deg between the two vectors and have a normalized B-normal at the center point of no more than 0.042. The final test score indicates that the cross product worked just as well or better as MVAB-0 for calculating tilt angles and predicting propagation delay times, although on some days the MVAB-0 method could do better.

[28] A comparison of phase front angle calculations from both the MVAB-0 and cross-product methods is shown in Figure 2. The three components of the IMF measured by the ACE spacecraft on 2 July 1999 are illustrated in the bottom three panels. The top two panels in the graph are the latitude and longitude of the PFN angles, using a convention similar to one that has been often used in the past for solar wind data sets. A PFN vector with zero longitude points toward the Earth along the $-X_{GSE}$ axis. The longitude has the same sign as the Y_{GSE} component of the vector and is derived from the arctangent of $Y/-X$. The latitude is the arcsine of the Z_{GSE} component so that positive latitude is pointing toward north.

[29] The tilt angles determined from the MVAB-0 method are shown with the red diamond symbols, and the associated eigenvalue ratios are shown with the red lines in the third row from the top. The MVAB-0 method is using its optimal parameters so that only points having eigenvalue ratios greater than 7.8 (the horizontal dashed line in third row) have their tilt angles plotted. As discussed earlier, the tilt angle of the PFN also needs to be less than the "limiting angle" of 75° to be selected. Twenty-five points of the 16-s ACE data are used for each variance matrix calculation, centered on each 16-s sample in the 24-h period.

[30] The normal angles that are calculated with the cross-product method are marked with the blue squares on the angle plots. For these cross-product calculations the IMF data are first smoothed with a 19-point sliding average, which serves as a low-pass filter. The two vectors for the cross product are located at times that are separated by plus and minus four samples (times 16-s) from the center. PFN calculations from the cross product are accepted only if: (1) the normalized magnetic field in the direction of the PFN (B-normal) must be less than 0.042, as illustrated with the blue lines in the fourth row on the plot, (2) the rotation or "spreading" angle, ω, between the two vectors is greater than or equal to 8.8°, as graphed in the fifth row, and (3) the PFN has an angle less than 75° relative to the solar wind flow. The times at which each cross-product calculation passes the selection are also marked with the vertical, light gray lines on the bottom three panels.

[31] The two panels in the top of Figure 2 show that the tilt angles from the two techniques are most often in

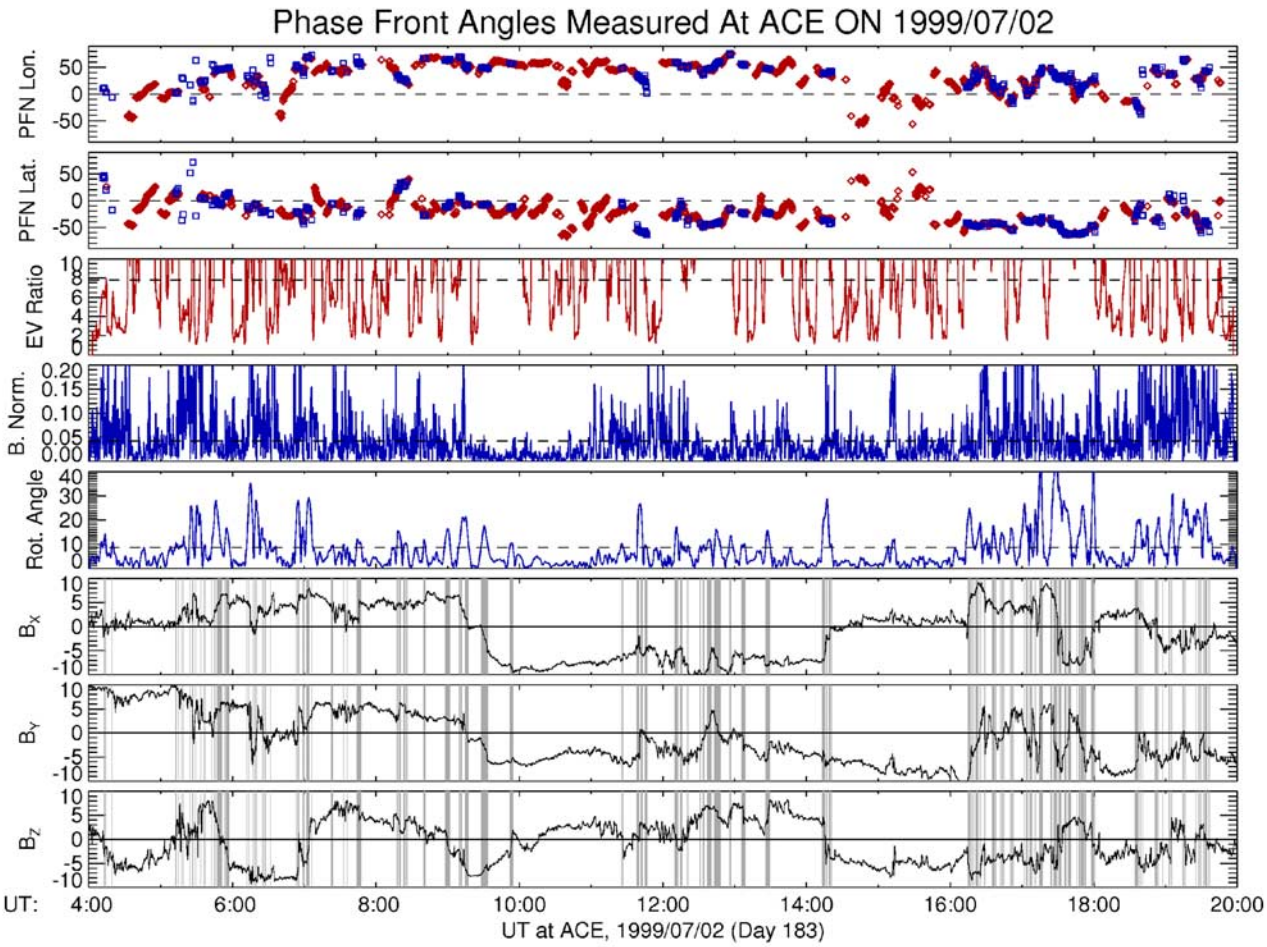

Figure 2. Example of separate IMF phase front normal angle calculations on 2 July 1999. The top two panels in the graph are the latitude and longitude angles of the phase front normal angles, with the angles from the MVAB-0 method shown with the red diamond symbols, and angles from the cross-product method indicated with the blue squares. The third row shows the minimum variance eigenvalue ratios, while the next two panels show the B-normal and rotation angle results from the cross products. The three components of the IMF measured by the ACE spacecraft are plotted in the bottom three panels, and the vertical, light gray lines mark the times at which each cross-product calculation passes the selection.

complete agreement, although there are also points where they deviate from each other. There are also times at which one method had results that passed its selection criteria for a valid measurement, while the other method did not.

8. A Combination of Methods

[32] The results shown in Figure 2 indicated that when the two methods did not agree, one of the two methods usually had surface-normal vector results that significantly deviated from the local trend. This observation led to the speculation that the best predictions might be obtained by doing a simultaneous calculation using both the MVAB-0 and cross-product methods, and keeping the results only where the two results (PFN directions) are in close agreement. Since the MVAB-0 method guarantees that B-normal is zero, then the B-normal test of the cross-product calculation is superfluous and hence would not be needed. Additionally, *Knetter et al.* [2004, p. 2] had stated:

> The other parameter affecting the reliability of MVA is the discontinuity spreading angle ω, i.e., the angle between the magnetic field vector upstream and downstream of the discontinuity. The bigger this angle, the smaller the error [*Lepping and Behannon*, 1980]. This is rather obvious since for large ω the discontinuity will be more clearly distinguished from the natural noise and superposed wave fields. Note that the importance of ω regarding MVA error analysis has often been disregarded in the past. In this paper we will show that ω is important in this context and we will specify a lower limit for ω to ensure safe use of MVA.

[33] In the combination of the two techniques, the cross-product method provides the measurement of the spreading angle, ω.

[34] Further tests with the two methods combined together led to some changes in the optimal parameters: 21 points for the MVAB-0 calculation, with the cutoff for the eigenvalue

Table 1. Optimal Parameters for the Minimum Variance (MVAB-0), Cross Product (CP), and Combined (CPMV) Tilt Angle Calculation Methods[a]

Method	N MV	EV Ratio	N Ave.	N Step	ω, deg	Max. B-norm.	θ, deg	Score, nT^2
MVAB-0	25	7.8						2.624
CP			19	4	8.8	.042		2.615
CPMV	21	1.1	11	8	9.8		9.9	2.598

[a]The columns give the number of numbers for the minimum variance matrix, eigenvalue cutoff ratio, number of points for sliding average prior to cross-product calculation, cross-product step size, spreading angle (ω), maximum B-normal, agreement angle (θ), and the test score using the mean square error.

ratio of only 1.1, and the cross product was computed from vectors at plus and minus 8 points, using an 11-point presmoothing, with a minimum spreading angle ω reduced of 9.8°. The "close agreement" between the two methods worked out to be within 9.9° of each other, as computed with a vector dot product of surface normals and determined with the iterated search for the best score. The values for the two angles were tested at 0.1° increments. An improved test score, 2.598 nT^2, was obtained by the combined method over each technique alone. As the two methods are doing cross checks on each other, the eigenvalue test is significantly relaxed, and the rotation angle requirement ensures that there is a sufficiently large enough change in the IMF direction to count as a significant phase surface passage rather than a noise fluctuation. A summary of the optimal parameters and test scores for each of the three methods is given in Table 1. These values are for IMF measurements with a 16-s cadence and would need to be changed for other data resolutions.

[35] The results of the PFN calculations using the combination of methods are shown in Figure 3, using the revised, optimal parameters. The format of the graph is very similar to that of Figure 2, except that the tilt angles in the top two panels are shown as blue squares connected with

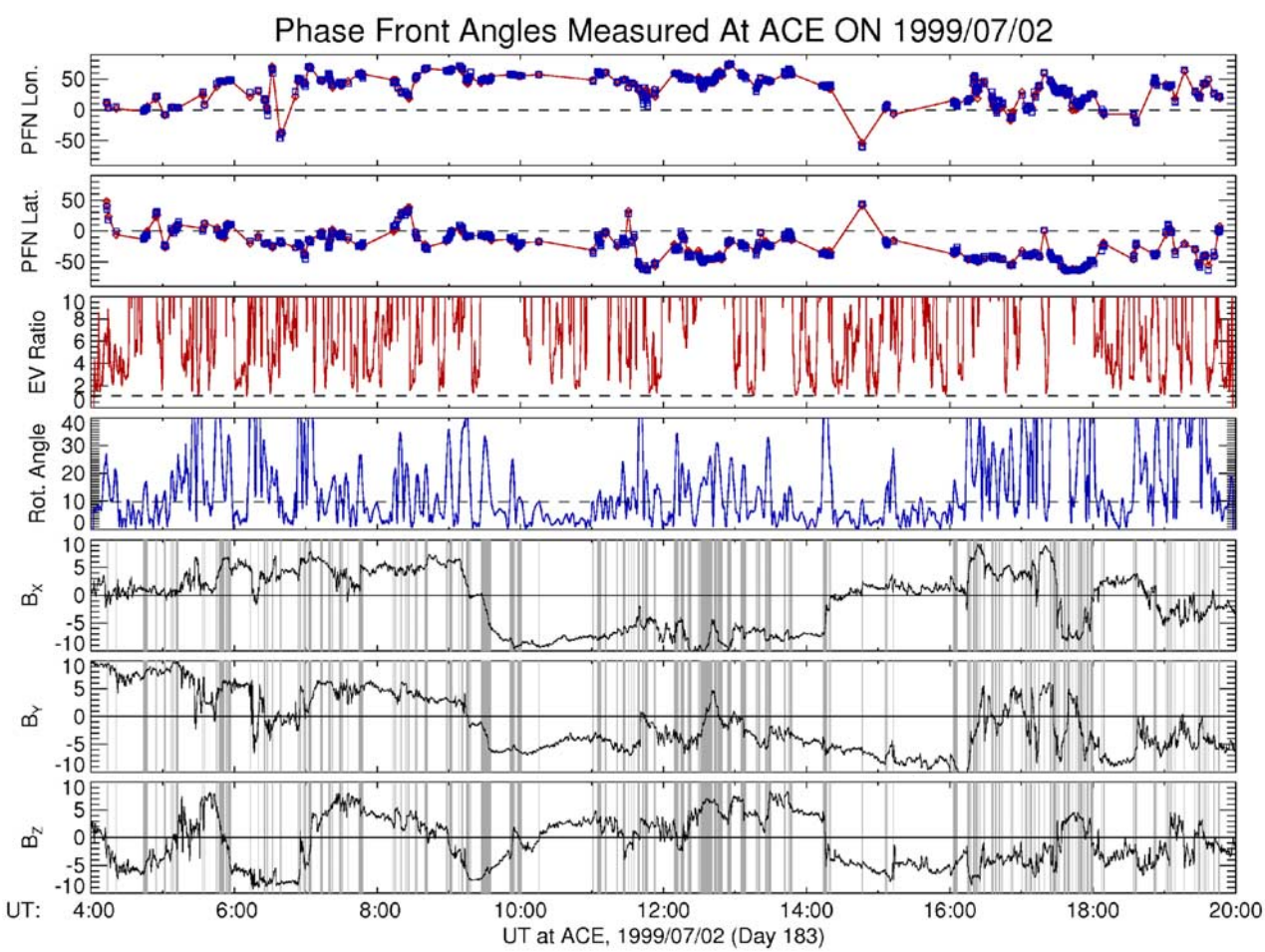

Figure 3. Example of IMF phase front normal angle calculations on 2 July 1999 from the combined MVAB-0 and cross-product method. The format is the same as in Figure 2, except that the phase front normal angle results from the combined method are plotted with blue squares connected with red lines, and the row with the B-normal values has been removed.

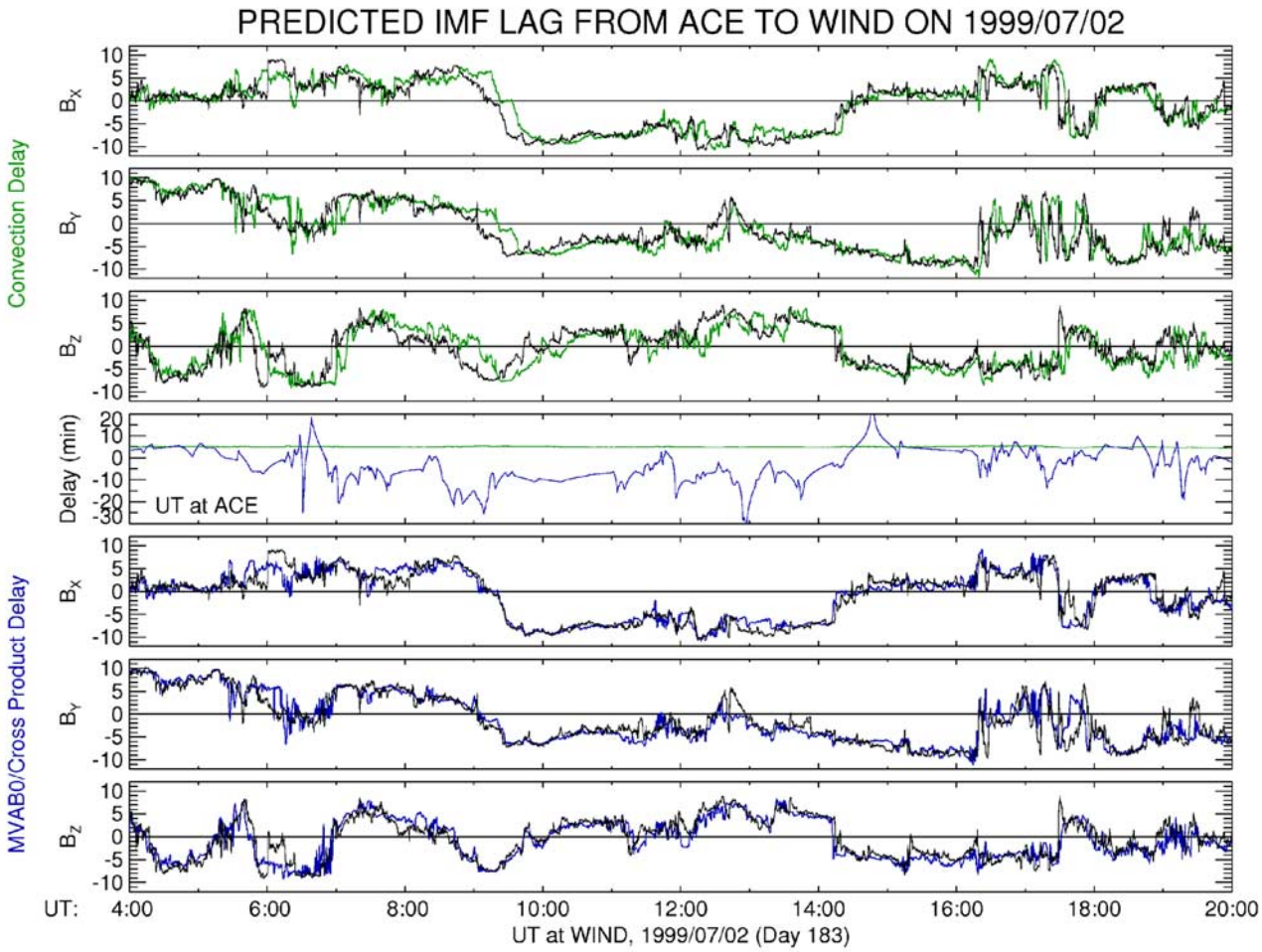

Figure 4. Comparison of the IMF measurements from both the Wind and ACE satellites, taken on 2 July 1999. The top three panels show the three components of the IMF measured at Wind in black, while the green lines show the ACE measurements, after first shifting these data in time according to a nontilted plane propagation at the observed solar wind velocity. The horizontal axis shows the UT at Wind. The delay time that was used is shown as the green line in the middle plot, plotted as a function of the UT at ACE. The bottom three panels show the same Wind data (black), but this time the ACE measurements (blue) have been shifted in time according to the tilt angles from the combined MVAB-0/cross-product technique. The values of these time shifts are shown in blue in the middle panel.

red lines. The blue squares are located where the two methods agree. The B-normal graph has been removed from the graph, as this test is no longer used or needed, as mentioned earlier. As before, the times at which each calculation passes the combined selection tests are marked with the vertical, light gray lines on the bottom three panels, superimposed over the IMF vector components. One point of significance is at about 1515 UT, where just a couple points at an IMF transition were selected, while there were none for a period before and afterward. This is a desired result, as wild fluctuations in the tilt angle are not wanted during intervals when there is a relatively unchanging IMF.

[36] Figures 4 and 5 show the results of using the combined method for calculating the propagation time delays from ACE to the Wind and Geotail spacecraft. The black lines in the top and bottom three panels in each figure show the IMF measured at the "target" spacecraft, as a function of UT at that spacecraft. In the top three panels the superimposed green lines show the IMF measured at ACE after applying a straight line convection delay to the target, using observed speeds but without any tilting of the phase surfaces with respect to the direction of propagation. The delay time that was used is shown with the green line in the middle row, as a function of UT at ACE rather than at the target. For comparison the blue line in this middle row shows the delay obtained with the tilted phase surface calculations, and the time-delayed ACE data are shown with the blue lines in the bottom three panels. There are many IMF features that do not line up properly in the top panels that do match in the bottom panels, particularly between 0900 and 1100 UT. For the comparison shown in Figure 4, the Wind spacecraft is located at approximately the same GSE X coordinate as ACE (208 and 238 R_E), so that the untilted-surface delay is only about 5 min. However, owing to a separation distance of 61 R_E in the Y direction the delay from ACE to Wind was affected by the tilting of

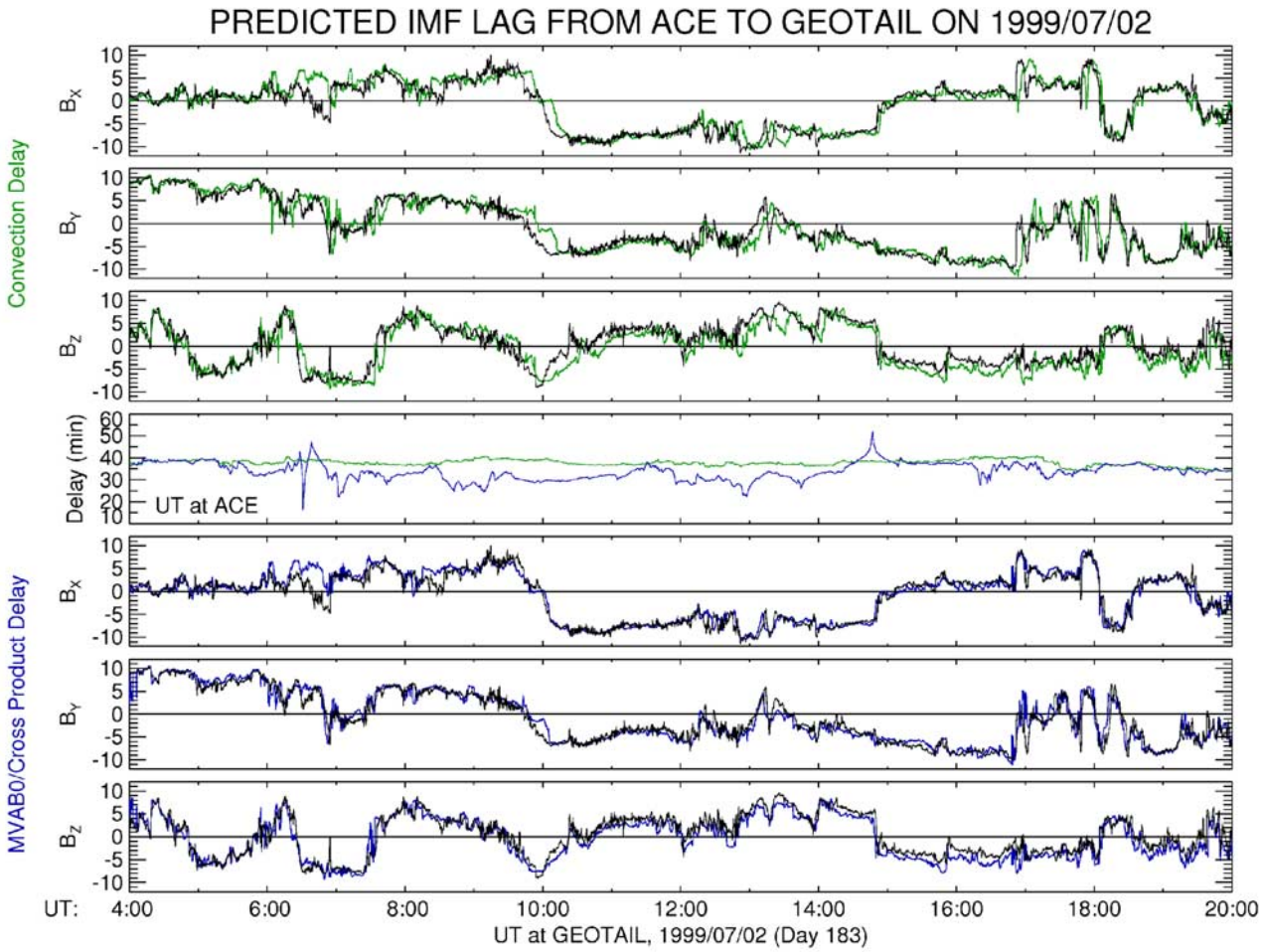

Figure 5. Comparison of the IMF measurements from both the Geotail and ACE satellites for the same case on 2 July 1999. The format is the same as in Figure 4, but with the black lines representing the Geotail measurements. The data are plotted as a function of UT at Geotail, with the exception of the middle panel which shows the time delays at ACE.

the phase surfaces in the Y direction, causing some IMF features to arrive at Wind up to 20 min earlier than at ACE, rather than 5 min later. As the separation between ACE and Geotail was only 19 R_E in the Y direction, the delay between them was affected by about 10 to 15 min (Figure 5). *Collier et al.* [2000] also show an example of an upstream spacecraft observing solar wind features after the downstream spacecraft, in their Figure 8.

[37] A comparison of test scores from the different methods is given in Tables 2 to 4, including the uncorrected, nontilted propagation method. Each of these three tables corresponds to the results obtained by propagating the IMF from ACE to the Wind, IMP-8, and Geotail spacecraft. The scoring is done for 38 d (33 for Geotail), and a point-for-point comparison at the target spacecraft is done for all IMF measurements between 0100 and 2300 UT on each day. The error difference between each of the three vector components has been squared and summed for all points in the day, and then the sum has been divided by the number of compared vectors times three, producing a mean square error, in nT^2, for each day. These tables also provide the year, month, and day for each test as well as the mean separation distances (ΔX, ΔY, and ΔZ) between ACE and the target spacecraft in units of R_E GSE. There are only 33 d used for the Geotail spacecraft (Table 4) as there were problems with the IMF measurements (i.e., data spikes, or within in the bow shock) during part of five of the days used in this set.

[38] Each row in these tables has an asterisk by the score that is the best for each day. At the bottom of each table are given the totals of the mean square error for all days and the mean for all days. Given at the bottom of the tables are the number of days that each propagation method had the best score, a count of the asterisks above. The last three panels have the winning counts in a one-on-one comparison between the three tilted-propagation methods. In all cases the nontilted propagation never had the best score, and in all three tables the combined method (CPMV) always had the lowest mean for the total. All three methods do produce a significant improvement over not using any tilt angle calculations at all, although it might not appear large due to the averaging over all points in the comparison, which includes periods when the IMF is not changing. Owing to

Table 2. Test Scores for Propagation From the ACE to Wind Spacecraft[a]

Year	M	D	No Tilt, nT^2	MVA, nT^2	CP, nT^2	CPMV, nT^2	ΔX, R_E	ΔY, R_E	ΔZ, R_E
1998	5	12	5.74	4.64*	4.72	4.71	17.3	−41.3	−50.1
1998	5	22	4.38	3.60	3.20*	3.58	25.8	−42.4	−50.9
1998	5	23	6.07	3.61*	3.94	3.73	27.0	−42.4	−50.6
1998	6	3	7.21	5.02*	5.29	5.12	46.4	−41.7	−41.9
1998	6	6	14.71	9.25	10.02	9.15*	54.2	−41.5	−40.0
1998	6	7	9.78	8.15	8.13	7.43*	57.2	−41.4	−39.3
1998	6	8	2.66	1.79*	1.90	1.87	60.3	−41.4	−38.5
1998	6	18	1.99	1.69	1.28*	1.86	104.7	−40.4	−26.5
1998	6	19	8.51	6.04	5.58*	5.97	110.9	−40.2	−24.9
1998	6	27	1.39	1.06*	1.08	1.10	182.2	−31.1	−9.4
1998	7	14	0.96	0.71	0.75	0.68*	151.5	1.4	8.6
1998	7	15	0.66	0.29*	0.31	0.30	154.6	−1.4	9.3
1998	8	8	0.40	0.28*	0.30	0.29	158.8	10.6	23.9
1998	8	20	5.24	3.53*	3.69	3.72	184.4	48.2	28.3
1998	8	23	9.48	6.65*	6.97	6.95	152.7	37.6	30.8
1998	9	3	2.05	1.07	1.00*	1.10	90.7	−1.5	33.1
1998	9	10	1.64	0.97	0.94	0.93*	71.4	−19.9	30.8
1998	10	11	1.13	0.84	0.81	0.78*	87.6	−62.1	−2.6
1998	10	20	7.02	3.99	3.94	3.73*	143.8	−71.3	−13.5
1998	10	21	6.27	3.77*	3.91	4.12	154.1	−71.9	−14.3
1998	10	31	1.62	1.17	1.17	1.14*	148.1	−30.9	−23.5
1998	11	1	1.87	1.24	1.27	1.19*	142.6	−32.4	−24.7
1998	11	12	2.40	1.19*	1.21	1.22	189.4	−33.9	−23.1
1999	4	29	3.94	2.81	2.73*	2.83	171.6	−3.2	−7.4
1999	4	30	2.53	2.06	2.04	1.88*	172.9	−5.2	1.3
1999	6	1	2.72	1.87*	1.93	2.03	48.1	41.4	−9.0
1999	6	5	1.60	1.45	1.53	1.35*	38.6	45.4	−8.1
1999	6	6	1.26	0.96*	1.06	0.99	36.7	46.5	−7.9
1999	6	15	3.27	2.80	2.11*	2.23	25.9	55.4	−5.7
1999	6	16	5.60	3.52	3.51*	3.55	25.3	56.2	−5.4
1999	6	17	4.85	3.33*	3.61	3.54	24.8	57.0	−5.1
1999	7	1	2.54	2.21	1.99	1.92*	27.6	61.6	−1.1
1999	7	2	7.59	5.05*	5.11	5.09	28.5	61.3	−0.8
1999	7	11	1.48	0.88	0.78	0.73*	39.5	54.8	2.0
1999	7	12	2.87	2.47	2.23*	2.39	41.2	53.6	2.3
1999	7	13	1.40	0.89*	0.92	0.92	42.9	52.3	2.6
1999	7	14	0.90	0.52	0.52	0.50*	44.7	50.9	2.9
1999	7	24	2.94	1.93*	2.00	1.98	68.3	29.9	6.0
Total			148.70	103.30		103.44	102.61		
Mean			23.91	2.72		2.72	2.70		
Score counts			0	17		8	10		
CP versus CPMV						14	24		
MVA versus CPMV				21			17		
MVA versus CP				23		15			

[a]The mean square error in nT^2 is given for each of four propagation methods, including not using any PFN tilt angles. Also included are the separation distances between the spacecraft in the X, Y, and Z GSE directions. The asterisks indicate which method had the best (lowest) score on each day.

the fact that on a day to day basis the IMF has different characteristics; on some days one method might produce better results than on other days. Interestingly, the combined CPMV method does not always have the largest number of days with the best score. Since it does always have the lowest mean score, this indicates that when the combined method produces a lower error it does so by a larger margin, and on the other days it is closer to a tie.

[39] Alternative methods for dealing with "out-of-sequence arrivals" were mentioned in section 5. Tables 2 to 4 have been produced with the method that produces the best score, which is to simply sort and resample, by averaging, the propagated IMF. For a direct comparison with the results shown in Table 3, the IMP-8 results have been calculated using the alternative methods. Giving precedence to IMF measurements that overtake ones that had been earlier in sequence results in a total score of 106.12 nT^2, compared to 93.03 nT^2 for the best method. Not allowing any overlap to occur (i.e., rejecting later-arriving phase fronts) resulted in a score of 103.86 nT^2. Counting the number of days with the better scores, the sort and average method was better on 29 d, and the other two methods were split at 5 and 4.

[40] The errors have been compared with the separation distance in the Y-Z directions. The results indicate that below 45 R_E separation the errors are scattered around the lower end of their range but start to increase when the separation is in the range of 45 to 60 R_E, beyond which there are few data.

9. Discussion

[41] It is emphasized that the techniques and parameters reported here are intended for use as a tool for routine processing of continuous IMF measurements, rather than discontinuity analysis. This processing could be done either with a real-time data stream, such as that from the ACE satellite or for producing an archive of IMF data with the

Table 3. Test Scores for Propagation From the ACE to IMP-8 Spacecraft[a]

Year	M	D	No Tilt, nT^2	MVA, nT^2	CP, nT^2	CPMV, nT^2	ΔX, R_E	ΔY, R_E	ΔZ, R_E
1998	5	12	2.43	1.94*	1.99	2.02	192.7	−38.8	−11.6
1998	5	22	3.36	2.48	2.63	2.30*	204.1	5.7	−36.8
1998	5	23	5.37	3.20*	3.28	3.32	192.8	−3.2	−26.9
1998	6	3	9.27	6.18	6.08*	6.20	205.3	26.0	−33.8
1998	6	6	5.24	4.53	4.47*	4.58	191.6	−2.2	−2.5
1998	6	7	6.11	5.06	4.90*	5.12	200.4	−11.3	3.8
1998	6	8	1.03	0.67*	0.71	0.77	213.3	−17.1	5.8
1998	6	18	1.34	1.12*	1.28	1.21	193.1	17.1	4.5
1998	6	19	9.76	6.78*	7.39	6.91	202.5	5.0	10.6
1998	6	27	4.12	2.69*	2.78	2.89	217.6	60.5	−18.8
1998	7	14	2.00	1.52*	1.54	1.61	210.9	21.6	30.1
1998	7	15	0.84	0.36*	0.41	0.38	222.6	11.2	27.4
1998	8	8	0.72	0.36	0.37	0.34*	219.6	8.1	43.0
1998	8	20	3.69	2.50	2.41	2.33*	217.7	2.1	47.4
1998	8	23	9.30	6.82	6.55	6.41*	246.8	−24.0	20.9
1998	9	3	2.12	1.32	1.27*	1.38	222.7	−31.3	33.6
1998	9	10	1.43	1.26	1.21	1.19*	245.1	18.8	35.5
1998	10	11	1.34	1.00	0.93	0.89*	225.6	−62.8	−14.3
1998	10	20	3.30	2.12*	2.13	2.16	199.8	−25.5	10.7
1998	10	21	3.40	2.44*	2.50	2.53	196.4	−38.3	−0.4
1998	10	31	0.86	0.68	0.72	0.67*	209.9	−2.8	9.3
1998	11	1	0.53	0.48	0.48	0.47*	197.4	−10.3	2.8
1998	11	12	5.25	4.46	4.35*	4.40	214.0	11.2	3.4
1999	4	29	7.33	3.77	3.64	3.62*	206.1	−50.9	9.0
1999	4	30	5.30	4.00	3.82	3.49*	218.7	−54.1	10.6
1999	6	1	2.90	2.33	2.20*	2.26	201.6	43.7	−23.2
1999	6	5	1.29	1.15	1.15	1.12*	201.0	4.0	7.5
1999	6	6	0.88	0.73	0.73	0.72*	212.2	−3.6	6.8
1999	6	15	3.11	2.39	1.91*	2.01	197.5	47.7	1.8
1999	6	16	5.55	3.76*	3.78	3.77	196.8	35.7	9.5
1999	6	17	5.92	4.56	4.45*	4.49	201.1	23.5	13.6
1999	7	1	1.30	1.22	1.14	1.09*	215.7	12.9	20.9
1999	7	2	3.92	3.05*	3.20	3.15	227.3	5.4	14.4
1999	7	11	0.83	0.57	0.44*	0.50	209.3	46.4	30.6
1999	7	12	2.90	2.56	2.27*	2.38	208.7	32.4	33.4
1999	7	13	1.12	0.74	0.72*	0.76	212.4	18.8	32.4
1999	7	14	0.77	0.45	0.47	0.44*	219.9	7.5	27.7
1999	7	24	4.39	3.23	3.23	3.16*	212.5	34.1	42.3
Total			130.33	94.49		93.53	93.05		
Mean			3.43	2.49		2.46	2.45		
Score counts			0	12		11	15		
CP versus CPMV						18	20		
MVA versus CPMV				17			21		
MVA versus CP				17		21			

[a]The format is the same as in Table 2.

time delays to the Earth's magnetosphere already included. This type of data base could be useful for various scientific studies of solar wind-magnetosphere coupling or substorm triggering, and one is already in production at NASA Goddard Space Flight Center using the techniques described here (see http://omniweb.gsfc.nasa.gov/omsc_min.html).

[42] IMF data from multiple spacecraft on 38 d were used to find the parameters that produced the best overall results for a variety of IMF conditions. The parameters listed in Table 1 should be considered as suggestions rather than absolute. As the characteristics of the IMF may change from quiet and steady to highly variable on a daily basis, one choice of parameters may work better on some days and different parameters work better on others. Parameters may be varied depending on a need or preference for more or less variability in the time delays or sensitivity to small-scale IMF transitions.

[43] The mean error test scores appear to have a low variability due to the fact that the corrections to the time delay propagation only have an effect at the minority points surrounding the IMF transitions having PFN directions that are tilted away from the solar wind velocity. An alternative method for testing the PFN calculations and delay corrections is to gather a set of IMF sequences that are known to have large timing errors when nontilted propagation is used. If the delay timing errors in such cases are measured (in seconds) rather than the mean IMF square error, then the methods discussed here would certainly produce a more impressive relative score. However, for the purpose of testing the various techniques and parameters, the method employed here helps to ensure that the delay predictions at other times are not made worse and also avoids some biases that could arise in constructing the test suite and measuring the timing.

[44] The IMF transitions that are detected by the described methods are assumed to be tangential in nature, although we hesitate to call them tangential discontinuities (TD), since historically the word "discontinuity" has been reserved for a more distinct class of events. However, in the traditional definition of a TD the magnetic field has no component along the discontinuities' normal vector. A TD-like transition is implicitly implied by application of the

Table 4. Test Scores for Propagation From the ACE to Geotail Spacecraft[a]

Year	M	D	No Tilt, nT^2	MVA, nT^2	CP, nT^2	CPMV, nT^2	ΔX, R_E	ΔY, R_E	ΔZ, R_E
1998	5	12	3.32	2.81*	2.86	2.83	209.8	−46.1	−17.6
1998	5	22	2.24	1.71*	1.89	1.72	205.5	−25.5	−19.9
1998	5	23	3.86	2.60	2.67	2.54*	211.5	−37.5	−20.1
1998	6	3	5.35	4.96	4.77*	4.79	213.5	−22.8	−19.6
1998	6	7	6.81	5.73*	5.79	5.92	201.8	−5.0	−17.0
1998	6	8	3.97	3.02*	3.12	3.25	209.1	−14.4	−17.5
1998	6	18	0.95	0.85*	0.89	0.86	204.8	3.2	−11.8
1998	6	19	10.09	7.08*	7.54	7.09	216.3	−1.6	−12.7
1998	6	27	4.19	3.27*	3.27	3.28	209.5	35.9	−5.3
1998	7	14	2.30	1.57*	1.72	1.67	207.4	28.3	7.9
1998	7	15	0.73	0.49	0.50	0.48*	216.9	19.3	7.0
1998	8	8	0.64	0.60	0.58*	0.59	221.1	38.1	24.3
1998	8	20	4.59	3.21	2.89	2.77*	219.1	10.2	25.4
1998	9	3	1.64	1.13	1.07*	1.20	229.0	14.1	26.4
1998	9	10	1.20	0.95	0.92	0.92*	218.3	−12.4	21.3
1998	10	11	0.81	0.74	0.73*	0.74	211.3	−22.0	0.5
1998	10	21	2.79	2.16*	2.24	2.38	213.3	−12.1	−6.7
1998	10	31	1.26	1.02*	1.06	1.03	217.0	−0.9	−13.1
1998	11	1	1.32	1.02	1.05	1.00*	206.6	−9.0	−15.6
1998	11	12	2.13	1.43	1.41*	1.43	204.6	−5.8	−21.9
1999	4	30	4.27	4.01	3.58*	3.85	220.9	−48.9	−14.4
1999	6	1	1.43	1.30	1.26*	1.30	217.3	−8.5	−19.8
1999	6	5	1.95	1.57	1.61	1.49*	207.3	9.9	−16.6
1999	6	6	1.18	0.92	0.97	0.89*	214.6	−1.4	−17.5
1999	6	15	5.14	3.24	2.88*	3.03	211.3	30.9	−11.1
1999	6	16	4.50	3.14*	3.39	3.39	210.9	15.1	−11.1
1999	6	17	4.37	3.49*	3.89	3.60	220.8	8.2	−12.3
1999	7	1	6.69	6.41	6.33	5.98*	212.4	33.5	0.7
1999	7	2	5.15	3.79*	3.82	3.82	214.0	19.4	0.1
1999	7	11	6.42	7.33	5.09*	5.24	222.3	40.8	8.7
1999	7	12	2.94	2.66	2.47*	2.51	215.5	25.6	8.7
1999	7	13	1.29	0.97	0.97*	0.98	221.5	14.6	7.5
1999	7	24	2.60	1.96*	2.07	2.03	228.7	6.1	14.0
Total			108.09	87.12		85.30	84.61		
Mean			3.28	2.64		2.58	2.56		
Score counts			0	14		11	8		
CP versus CPMV						16	17		
MVA versus CPMV				18			15		
MVA versus CP				19		14			

[a]The format is the same as in Table 2.

cross-product method [*Knetter et al.*, 2004]. TDs also do not propagate through the solar wind plasma but are advected with it, which is a necessary condition for being able to use the solar wind's velocity in order to predict the IMF transitions' arrival times. On the other hand, it is desirable for our methods to ignore rotational discontinuities (RD), which do have a magnetic field component in the normal direction, as they propagate through the solar wind plasma [*Neugebauer*, 2006]. Historically, IMF transitions were at one time assumed to be mostly RDs, whereas more recent multispacecraft observations have led to the conclusion that the majority of discontinuities are tangential [*Horbury et al.*, 2001; *Knetter et al.*, 2004]. On the other hand, *Neugebauer* [2006] contends that there is no clear answer to the question of relative abundances. *Tsurutani et al.* [2007] suggest that many directional discontinuities are kinetic structures, such as phase steepened edges of Alfven waves, rather than pure TDs.

[45] The rotation of the magnetic field that is detected by the vector cross product is presumed to be caused by currents within the IMF transition. The requirement that this "spreading angle" must exceed some minimum value puts a lower limit on the magnitude of the current for it to be considered important, thereby filtering out the small-scale, low-magnitude noise fluctuations. The use of a number of points spanning over 5 min of time for the calculations also selects for only the large-scale transitions. Yet the rotation angle may be small in places where the MVAB-0 method passes the eigenvalue ratio test; as mentioned earlier, the EV ratio is not always a good discriminator for the small-scale noise. Keep in mind that the development of MVA techniques have involved the detailed analysis of satellite magnetopause crossings or very distinct "directional discontinuities" in the IMF, which have been said to occur at a rate of only one or two per hour. Most likely these "discontinuities" occur at a multitude of scales from large to small, wherever there is a change in the IMF orientation. Finally, as pointed out by *Bargatze et al.* [2006], some other technique needs to be developed to handle interplanetary shocks and possibly RDs as separate classes of events. They suggest a set of multiple tools for providing comprehensive delay calculations.

10. Summary

[46] Changes in the IMF vectors often occur within surfaces that are tilted with respect to the direction of solar wind propagation, which causes the delay time of the IMF

transitions from one point to another to vary according to the degree of tilt and the separation distance in the perpendicular direction. For accurate delay calculations with real time IMF measurements, such as that from the ACE satellite, or for the creation of scientific data sets that include the calculated delays, it is necessary to be able to determine the phase surface orientation angles using the magnetic field measurements on one spacecraft only.

[47] In this study, methods for calculating this tilt angle have been tested for accuracy by a comparison with the angles measured by multiple satellites, using a data set comprised of measurements from 38 d. One method is a variation of the minimum variance of the magnetic field, constrained by the condition that the average field along the PFN is zero, known as MVAB-0. Another technique is to simply calculate the vector cross product between magnetic fields measured before and after each IMF transition and requiring that the angle of rotation within the transition exceeds some minimum. The choices of the different parameters for the calculation and error discrimination are important. An optimization of parameters was performed by testing how well the propagation delays from one spacecraft to another are predicted. The tests have indicated that, when optimized, both procedures work comparably well separately, and further improvements to time delay predictions are obtained by combining together both the MVAB-0 and cross-product techniques, where the results of both methods must be in near agreement. Any of these is significantly better than neglecting tilts. A primary result of the optimized parameters is the filtering of small-scale fluctuations.

[48] These methods implicitly assume that the IMF transitions are embedded within the solar wind plasma and moving at the same velocity. Rotational discontinuities are not handled and may not even be important as indicated by the good results obtained in predicting the IMF arrival at other spacecraft. On the other hand, prediction of the arrival of interplanetary shocks traveling faster than the solar wind would require the use of an auxiliary technique operating in parallel.

[49] The use of these tilt angle calculations to make predictions of IMF arrival at other locations requires the assumption that the IMF transition surfaces are flat over the scales of the flow-transverse separation distance between the observing satellite and the target location. Prior experience indicates that this is a reasonable assumption within the 40 R_E radius of the ACE orbit around the Earth-Sun line. For example, *Collier et al.* [2000] found that phase surfaces have radii of curvature on the order of 100 R_E. Beyond 40 to 60 R_E separation distances the curvature and finite scale of the phase surfaces are expected to have a more significant effect.

[50] The process of building target-location IMF time series without concern for out-of-sequence data packets yields better scores than eliminating some time-shifted data based on a priori expectations of how the phase surfaces should interact. That successive phase surfaces may not be parallel indicates that they must have finite dimensions or intersect at locations away from the observation point. A possible course for future research is to obtain a better understanding of the geometries of the IMF phase surfaces and how they interact with each other over large distances.

[51] **Acknowledgments.** This research was supported by NASA grant NNX07AC05G to Solana Scientific Inc. from the Sun-Earth Connections Guest Investigator Program. The authors thank the ACE, Wind, IMP-8, and Geotail PIs for use of the magnetometer and solar wind data. The ACE, Wind, and IMP-8 data were obtained through NASA's Space Physics Data Facility. Geotail magnetic field data were provided by S. Kokubun and T. Nagai through the Data Archives and Transmission System (DARTS) at the Institute of Space and Astronautical Science (ISAS) in Japan. The authors thank Lee Bargatze for useful discussions.Amitava Bhattacharjee thanks Gerard T. Blanchard and another reviewer for their assistance in evaluating this paper.

References

Bargatze, L. F., R. L. McPherron, J. Minamora, and D. Weimer (2005), A new interpretation of Weimer et al.'s solar wind propagation delay technique, *J. Geophys. Res.*, *110*, A07105, doi:10.1029/2004JA010902.

Bargatze, L. F., R. L. McPherron, J. Minamora, and D. Weimer (2006), Reply to comment by Haaland et al. on "A new interpretation of Weimer et al.'s solar wind propagation delay technique," J, *J. Geophys. Res.*, *111*, A06103, doi:10.1029/2005JA011557.

Borovsky, J. (2006), The flux-tube texture of the solar wind, *Eos Trans. AGU*, *87*(52), Fall Meet. Suppl., Abstract SH43C-05.

Burlaga, L. F. (1969), Directional discontinuities in the interplanetary magnetic field, *Sol. Phys.*, *7*, 54–71.

Collier, M. R., J. A. Slavin, R. P. Lepping, A. Szabo, and K. Ogilvie (1998), Timing accuracy for the simple planar propagation of magnetic field structures in the solar wind, *Geophys. Res. Lett.*, *25*, 2509–2512.

Collier, M. R., A. Szabo, J. A. Slavin, R. P. Lepping, and S. Kokubun (2000), IMF length scales and predictability: The two length scale medium, *Int. J. Geomagn. Aeron.*, *2*, 3–16.

Haaland, S., et al. (2004), Four-spacecraft determination of magnetopause orientation, motion and thickness: Comparison with results from single-spacecraft methods, *Ann. Geophys.*, *22*, 1347–1365.

Haaland, S., G. Paschmann, and B. U. Ö. Sonnerup (2006), Comment on "'A new interpretation of Weimer et al.'s solar wind propagation delay technique'' by Bargatze et al., *J. Geophys. Res.*, *111*, A06102, doi:10.1029/2005JA011376.

Horbury, T. S., D. Burgess, and M. Franz (2001), Three spacecraft observations of solar wind discontinuities, *Geophys. Res. Lett.*, *28*, 677–680.

Knetter, T., F. M. Neubauer, T. Horbury, and A. Balogh (2004), Four-point discontinuity observations using Cluster magnetic field data: A statistical survey, *J. Geophys. Res.*, *109*, A06102, doi:10.1029/2003JA010099.

Lepping, R. P., and K. W. Behannon (1980), Magnetic field directional discontinuities: 1. Minimum variance errors, *J. Geophys. Res.*, *85*, 4695–4703.

McComas, D. J., S. J. Bame, P. Barber, W. C. Feldman, J. L. Phillips, and P. Riley (1998), Solar wind electron, proton, and alpha monitor (SWEPAM) on the Advanced Composition Explorer, *Space Sci. Rev.*, *86*, 563–612.

Neugebauer, M. (2006), Comment on the abundances of rotational and tangential discontinuities in the solar wind, *J. Geophys. Res.*, *111*, A04103, doi:10.1029/2005JA011497.

Ridley, A. J. (2000), Estimations of the uncertainty in timing the relationship between magnetospheric and solar wind processes, *J. Atmos. Sol. Terr. Phys.*, *62*, 757–771.

Smith, C. W., M. H. Acuna, L. F. Burlaga, J. L'Heureux, N. F. Ness, and J. Scheifele (1998), The ACE Magnetic Field Experiment, *Space Sci. Rev.*, *86*, 613.

Sonnerup, B. U. Ö., and M. Scheible (1998), Minimum and maximum variance analysis, in *Analysis Methods for Multi-Spacecraft Data*, edited by G. Paschmann and P. W. Daly, pp. 185–220, Int. Soc. for Solid-State Ionics, Bern, Switzerland.

Sonnerup, B. U. Ö., S. Haaland, G. Paschmann, B. Lavraud, M. W. Dunlop, H. Rème, and A. Balogh (2004), Orientation and motion of a discontinuity from single-spacecraft measurements of plasma velocity and density: Minimum mass flux residue, *J. Geophys. Res.*, *109*, A03221, doi:10.1029/2003JA010230.

Tsurutani, B. T., G. S. Lakhina, O. P. Verkhoglyadova, E. Echer, and F. L. Guarnieri (2007), Comment on "Comment on the abundances of rotational and tangential discontinuities in the solar wind'' by M. Neugebauer, *J. Geophys. Res.*, *112*, A03101, doi:10.1029/2006JA011973.

Weimer, D. R. (2004), Correction to "Predicting interplanetary magnetic field (IMF) propagation delay times using the minimum variance technique,", *J. Geophys. Res.*, *109*, A12104, doi:10.1029/2004JA010691.

Weimer, D. R., D. M. Ober, N. C. Maynard, W. J. Burke, M. R. Collier, D. J. McComas, N. F. Ness, and C. W. Smith (2002), Variable time delays in the propagation of the interplanetary magnetic field, *J. Geophys. Res.*, *107*(A8), 1210, doi:10.1029/2001JA009102.

Weimer, D. R., D. M. Ober, N. C. Maynard, M. R. Collier, D. J. McComas, N. F. Ness, C. W. Smith, and J. Watermann (2003), Predicting interpla-

netary magnetic field (IMF) propagation delay times using the minimum variance technique, *J. Geophys. Res.*, *108*(A1), 1026, doi:10.1029/2002JA009405.

J. H. King, NASA Goddard Space Flight Center, Mail Code 672, Greenbelt, MD 20771, USA. (jking@mail630.gsfc.nasa.gov)

D. R. Weimer, Solana Scientific Inc., 11 Laurel Crest Drive, Brookline, NH 03033, USA. (weimer@solanasci.com)